STUDY OF THE CHARACTERISTICS OF MICROSILICA DUST GENERATED DURING FERROSILICON PRODUCTION

Doniyor Kholikulov[1], Shokhrukh Khojiev[1], Olmos Boltayev[1], Odiljon Abdurakhmonov[2], Saidalokhon Mutalibkhonov[1], Ikromjon Shaymanov[1]

[1]*Department of Metallurgy, Almalyk State Technical Institute Tashkent region Almalyk city, 45 Mirzo Ulugbek St. 110100, Uzbekistan, doniyor_xb@mail.ru (D.K.); hojiyevshohruh@yandex.ru (Sh.K.); boss.olmos@mail.ru (O.B.); mutalibkhonov1990@gmail.com (S.M.); ikromshaymanov5@gmail.com (I.Sh.).*

[2]*Department of "Technology of Silicate Materials and Rare Noble Metals", Tashkent, Tashkent Chemical-Technological Institute 32 A. Navoi St., 100011, Tashkent, Uzbekistan, odilzhon.abdurakhmonov@mail.ru (O.A.).*

Received 25 March 2026
Accepted 07 May 2026
DOI: 10.59957/jctm.v61.i5.2026.8

ABSTRACT

Microsilica dust generated during ferrosilicon production accumulates in substantial quantities, creating significant environmental concerns. However, its compositional and structural features enable its consideration as a valuable secondary raw material. In this study, technogenic microsilica obtained from ferrosilicon production waste in Uzbekistan was comprehensively characterized for the first-time using X-ray fluorescence (XRF), X-ray diffraction (XRD), Fourier-transform infrared spectroscopy (FT-IR), and transmission electron microscopy coupled with energy-dispersive spectroscopy (TEM/EDS). Its potential application as a functional filler was also evaluated. According to XRF analysis, silicon was identified as the dominant component, accounting for 50.6 wt. %. XRD results revealed a broad diffuse maximum within the 2θ range of 15-30°, indicating that the material predominantly exhibits an amorphous structure. FT-IR spectra demonstrated intense absorption bands characteristic of Si-O-Si bonds. TEM images showed that the particles possess a spherical morphology with sizes ranging from 50 to 200 nm and exhibit a pronounced tendency toward aggregation. EDS analysis confirmed that Si and O are the prevailing elements in the composition. The spherical morphology and nanoscale structure of the particles indicate that microsilica is formed in the vapor phase during ferrosilicon smelting and subsequently undergoes rapid condensation. The results demonstrate a clear relationship between the chemical composition of microsilica and its amorphous structural state, highlighting distinctive features of technogenic microsilica generated under the conditions of ferrosilicon production in Uzbekistan compared to conventional silica fume samples.

Keywords: microsilica dust, ferrosilicon production, physicochemical characterization, amorphous silicon dioxide, XRF analysis, XRD analysis, FT-IR spectroscopy, TEM analysis.

INTRODUCTION

Dust generated during metallurgical processes exerts a detrimental impact on the environment, contaminating the atmosphere, soil, and water bodies with metals and sulfur-containing compounds. Such emissions contribute to acid rain formation, vegetation degradation, and ecosystem accumulation, potentially leading to severe health disorders in humans, including silicosis and intoxication. According to the literature, 70 - 90 % of metallurgical dust consists of oxides, while the remainder includes ferrites, sulfates, sulfides, chlorides, and other compounds [1 - 6].

In recent years, the recycling of industrial waste as secondary raw materials and the production of high value-added products from such materials have become priority directions in both scientific research and industrial practice [7 - 9]. Metallurgical wastes are considered promising feedstocks due to their

high content of valuable components, despite their environmental burden [10, 11].

During ferrosilicon production, significant quantities of microsilica dust (microsilica, silica fume) are generated [12, 13]. This material forms primarily through the volatilization of silicon monoxide in high-temperature electric furnaces followed by rapid cooling and condensation [14, 15]. As a result, highly dispersed amorphous silicon dioxide particles are produced [10].

Mitov et al. have investigated the recycling of iron-containing metallurgical wastes through direct reduction processes in rotary furnaces at 1050 - 1150°C under reducing conditions [16]. Various iron ore pellets and coal powder were used, technological parameters were optimized, and iron-containing pellets meeting market requirements were successfully produced.

Microsilica is characterized by a high specific surface area, enhanced reactivity, and pozzolanic activity, enabling its application as a functional filler in construction materials, polymer composites, rubber, ceramics, and other fields [17 - 20]. However, its composition varies depending on the industrial source, necessitating comprehensive physicochemical investigations to accurately assess its properties [21, 22].

Experimental studies on nanofluids consisting of water and 16 nm SiO_2 nanoparticles have demonstrated that evaporation behaviour depends strongly on nanoparticle concentration [23, 24]. At concentrations up to 0.1 wt. %, nanoparticles reduce evaporation %, the rate stabilizes. These findings indicate that water evaporation can be controlled through nanoparticle concentration adjustment.

In another study, pure amorphous SiO_2 was synthesized from Kankara kaolinitic clay (Nigeria) using chemical extraction and the sol-gel method [25]. The clay was beneficiated, thermally activated, acid-treated, and subsequently processed with NaOH to obtain sodium silicate solution, which was precipitated using HCl. The resulting gel was dried to yield white SiO_2 powder.

Yokubov et al. investigated the mechanical properties of cement composites prepared using mixing water modified by SiO_2 nanosol of various compositions [26]. The mixing water was activated using acoustic (22 kHz, 4.0 W cm^{-2}) and electrochemical (15 V, 4.5 mA cm^{-2}) methods. The results demonstrated that nano-additives can enhance concrete strength by one grade.

The chemical composition, phase state, and structural characteristics of microsilica are key factors determining its application efficiency [27, 28]. Consequently, comprehensive characterization using modern analytical techniques such as XRF, XRD, FT-IR, and SEM/TEM has become widespread [29 - 33]. XRF analysis provides elemental composition data [34], XRD identifies amorphous or crystalline structural states [35], FT-IR confirms the presence of characteristic Si-O-Si bonds [36], and electron microscopy enables evaluation of particle morphology, size, and aggregation behavior [37 - 41].

Despite numerous studies on microsilica generated during ferrosilicon production, the structural features of technogenic microsilica formed under specific technological conditions remain insufficiently investigated. Comprehensive studies on microsilica dust generated under the conditions of ferrosilicon production in Uzbekistan are virtually absent in the literature.

In the present study, technogenic microsilica obtained from ferrosilicon production in Uzbekistan was comprehensively characterized using XRF, XRD, FT-IR, and TEM/EDS techniques. The influence of associated elements such as Ca, Fe, and Mn on the amorphous structure of silicon dioxide was analysed in detail. The results establish a correlation between chemical composition and structural state, providing scientific justification for the distinctive features of this material compared to conventional silica fume samples.

EXPERIMENTAL

Materials and methods

Microsilica dust generated in the ferrosilicon production workshop of JSC "Uzmetkombinat" was selected as the object of investigation. This microsilica is formed during ferrosilicon smelting in electric arc furnaces because of cooling high-temperature process gases and their subsequent capture in dust-collection systems. Therefore, the material is of technogenic origin, and its composition is directly determined by the specific technological conditions of the production process.

To ensure representativeness, several individual samples were collected from different points within the production workshop. These samples were combined under laboratory conditions and thoroughly homogenized by mechanical mixing. From the resulting composite mixture, a single integral sample was isolated

and used for subsequent laboratory analyses. This approach ensured reliable representation of the average chemical and structural characteristics of the material.

The obtained microsilica dust is a highly dispersed powder with a grayish-white appearance, characterized by a lightweight and fine structure. Its high dispersity and large specific surface area enhance its reactivity and enable its potential application as a functional filler in various industrial fields. Owing to its technogenic origin, microsilica may also be regarded as an environmentally significant secondary raw material.

The prepared sample was comprehensively characterized using XRF, XRD, FT-IR, and TEM/EDS analytical techniques. These methods enabled a detailed evaluation of elemental composition, phase state, chemical bonding, and morphological features.

A combination of modern instrumental techniques was employed for comprehensive characterization of the samples.

The elemental composition was determined using energy-dispersive X-ray fluorescence spectroscopy (EDXRF) with a Rigaku NEX CG II Series analyser (Japan). The instrument utilizes indirect excitation through secondary targets and polarized monochromatic radiation in a 90° Cartesian geometry, which enhances the signal-to-noise ratio and ensures low detection limits even for complex matrices.

The phase composition and crystalline structure were examined by X-ray diffraction (XRD) using a laboratory powder diffractometer. Measurements were performed with Cu - Kα radiation (λ = 1.5406 Å) at an accelerating voltage of 40 kV and a current of 30 mA in θ - 2θ geometry. Data were collected over a 2θ range of 5 - 70°, with a step size of 0.02° and a scanning rate of $2°\cdot min^{-1}$.

Structural bonds and functional groups were analysed using Fourier-transform infrared (FT-IR) spectroscopy with a Shimadzu FT-IR spectrometer equipped with an attenuated total reflectance (ATR) accessory. Spectra were recorded in the range of 4500 - 500 cm^{-1} with a resolution of 4 cm^{-1}. Each spectrum was averaged over 45 scans and processed in % transmittance mode using LabSolutions IR software.

The morphology, particle size, and microstructural features were investigated by transmission electron microscopy (TEM) and scanning transmission electron microscopy ((S)TEM) using a Thermo Fisher Scientific Talos F200i instrument (USA) equipped with a Bruker XFlash 6 - 30 EDS detector. TEM and STEM micrographs were used to assess particle shape, degree of aggregation, and size distribution. Elemental composition and spatial distribution were determined by point EDS spectra and elemental mapping.

RESULTS AND DISCUSSION

Initial raw material: Chemical and phase composition

The elemental composition of the initial microsilica dust was analysed by EDXRF. The obtained spectrum exhibited intense characteristic peaks corresponding to silicon (Si), confirming that SiO_2 constitutes the principal component of the sample. In addition, characteristic lines of aluminium (Al), magnesium (Mg), calcium (Ca), potassium (K), iron (Fe), and other minor elements were detected (Fig. 1). These results indicate that the microsilica dust represents a multicomponent technogenic material and confirm its origin as a by-product of metallurgical processes

According to the X-ray fluorescence (XRF) analysis, the microsilica sample represents a multicomponent technogenic material of silicate nature. In the quantitative composition, silicon (Si) exhibited the highest proportion, accounting for 50.6 wt. %. This confirms that the primary matrix of the sample is formed predominantly by silicon dioxide (SiO_2), which is characteristic of microsilica dust.

Calcium (Ca - 4.29 wt. %) was identified as the second most significant component, indicating the possible presence of calcium silicates or CaO-based mineral phases within the material. Additionally, the detection of potassium (K - 0.778 wt. %), magnesium (Mg - 0.645 wt. %), and aluminium (Al - 0.520 wt. %) supports the formation of aluminosilicate and alkali silicate phases. Such a compositional profile is typical of metallurgical industrial waste, particularly microsilica dust generated during ferrosilicon production.

The presence of metallic elements such as iron (Fe - 1.14 wt. %), manganese (Mn - 0.308 wt. %), zinc (Zn - 0.359 wt. %), and copper (Cu - 0.0156 wt. %) further confirms the metallurgical origin of the material. Iron suggests the possible occurrence of iron oxide phases, while manganese and zinc are likely present as technogenic impurities associated with the smelting process.

The detection of chlorine (Cl - 0.0858 wt. %)

and sulfur (S - 0.238 wt. %) may be attributed to fuel combustion products, the influence of the gas-phase environment, or natural impurities in the raw materials. Trace elements such as strontium (Sr), zirconium (Zr), lead (Pb), and tin (Sn) were identified in very small amounts and can be regarded as minor accompanying components that do not significantly affect the overall characteristics of the sample. Overall, the XRF results confirm that the microsilica sample is predominantly a SiO_2-based multicomponent silicate material. The presence of Ca, Al, Mg, and K suggests the formation of aluminosilicate phases, whereas Fe, Mn, and Zn reflect its metallurgical origin. This compositional profile indicates that the material is scientifically and technologically promising as a secondary raw material, particularly to produce amorphous silicon dioxide, the development of functional fillers, and applications in the construction materials industry (Fig. 2).

The XRD diffractogram exhibited a broad diffuse maximum within the 2θ range of 15-30°, indicating the absence of long-range crystalline order in the material. This feature is characteristic of amorphous structures and can be explained by the rapid cooling and condensation of SiO vapours formed in the high-temperature vapor phase during ferrosilicon smelting, resulting in the formation of amorphous SiO_2.

A similar amorphous halo has been reported by other authors for microsilica obtained from ferrosilicon production [8, 10]. However, in the present sample, the near absence of distinct crystalline reflections suggests

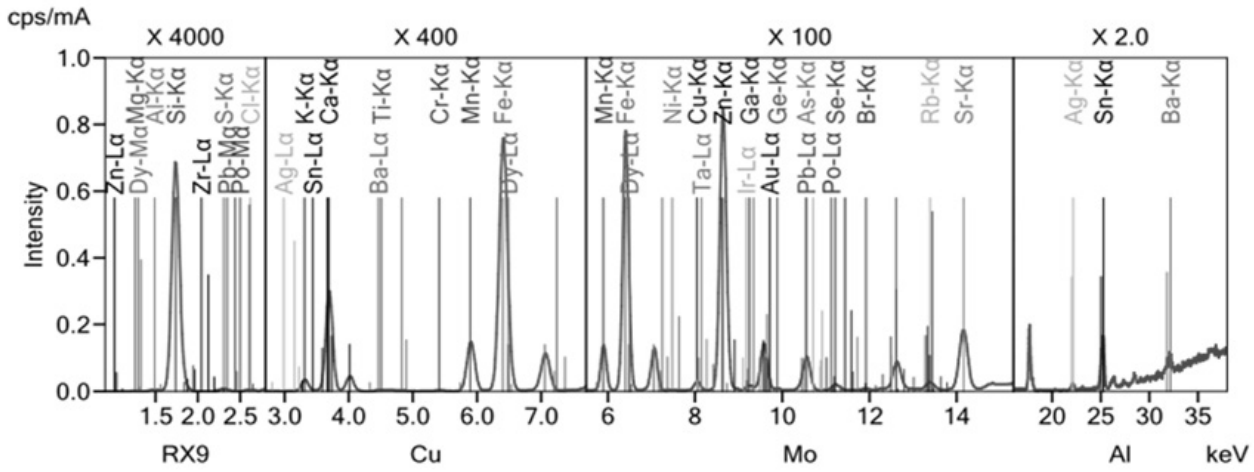

Fig. 1. XRF spectrum of the microsilica sample.

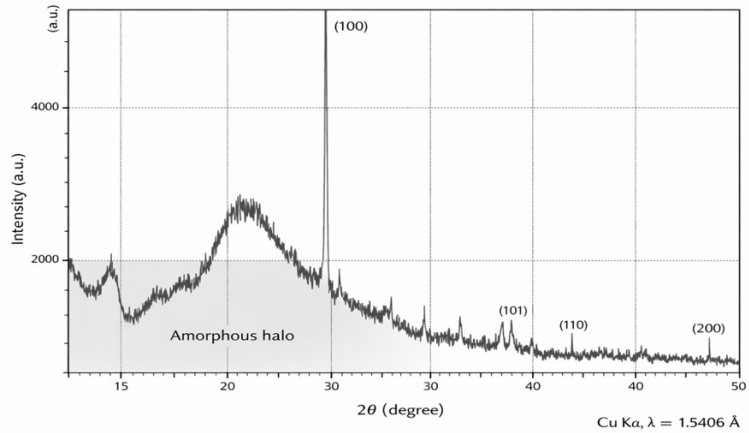

Fig. 2. X-ray diffraction pattern of the obtained sample showing a dominant amorphous halo (15-30° 2θ) and minor crystalline peaks, indicating the predominantly amorphous nature of the material.

a particularly high degree of amorphousness, which is a favorable characteristic for enhanced reactivity and potential pozzolanic activity. To determine the functional composition of the microsilica sample, ATR - FT-IR (Attenuated Total Reflectance - Fourier Transform Infrared Spectroscopy) analysis was performed. The spectrum was recorded in the range of 4500-500 cm^{-1} in transmittance mode.

The obtained results indicate that the chemical structure of the sample is predominantly characterized by bonds typical of silicon dioxide (SiO_2), confirming the silicate nature of the material (Fig. 3).

The FT-IR spectrum exhibited intense absorption bands at approximately 1100, 800, and 460 cm^{-1}, which are characteristic of amorphous silica and are fully consistent with the XRD results. In particular, the broad band centered around 1100 cm^{-1} corresponds to the asymmetric stretching vibrations of Si - O - Si bonds in a disordered (amorphous) network. This feature confirms that the silicon-oxygen tetrahedra are arranged without long-range periodicity, further supporting the amorphous nature of the material.

Such spectral characteristics have also been reported for silica fume samples investigated by other authors [9]. However, in the present case, the relatively low intensity of absorption bands associated with hydroxyl (-OH) groups indicates a comparatively low degree of surface hydration. This suggests that the material contains a limited amount of adsorbed water or silanol groups.

Compared with microsilica samples reported in the literature, the diffractogram of the material investigated in this study shows a particularly broad amorphous halo within the 2θ range of 15 - 30° [6 - 10]. This observation indicates a highly disordered SiO_2 structure with a significant number of structural defects. Such a structural state can be attributed to the rapid condensation of SiO vapours during ferrosilicon smelting, as well as to the presence of associated elements such as Ca, Fe, and Mn, which may disturb the silica network and inhibit crystallization.

The relatively low intensity of absorption bands corresponding to silanol (Si-OH) groups suggests that the surface of the microsilica particles is weakly hydroxylated. This feature may reduce the hygroscopicity of the material and enhance its compatibility in polymer and composite systems when used as a functional filler. These structural characteristics appear to be typical of technogenic microsilica and remain insufficiently discussed in the available literature.

The morphological, structural, and elemental characteristics of the microsilica sample were further investigated using electron microscopy and energy-dispersive X-ray spectroscopy (EDS). The TEM/SEM - EDS results were subjected to detailed scientific

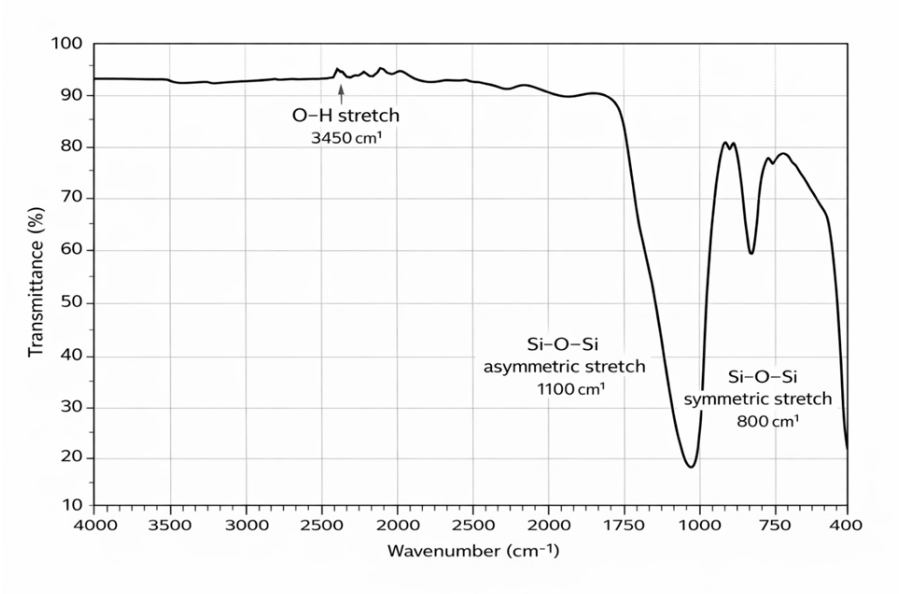

Fig. 3. ATR-FT-IR spectrum of the microsilica sample.

analysis.

Electron micrographs obtained at various magnifications enabled high-resolution characterization of the morphological features of the sample particles (Fig. 4).

TEM images revealed predominantly spherical particles within the size range of 50 -200 nm, which confirms the vapor-phase formation mechanism of microsilica. During ferrosilicon smelting, SiO vapours are generated at high temperatures and transition into the gas phase. Upon entering the cooling zone, these vapours undergo rapid condensation, resulting in the formation of spherical nanoparticles.

Due to the rapid cooling kinetics, insufficient time is available for crystallization, and the particles remain in an amorphous state. This observation is consistent with the XRD results, which demonstrated the absence of long-range crystalline order.

A similar spherical morphology has been reported in the studies of Zhong et al. and Liang et al [8, 10]. However, the relatively narrow particle size distribution observed in the present study (primarily 50 - 200 nm) suggests

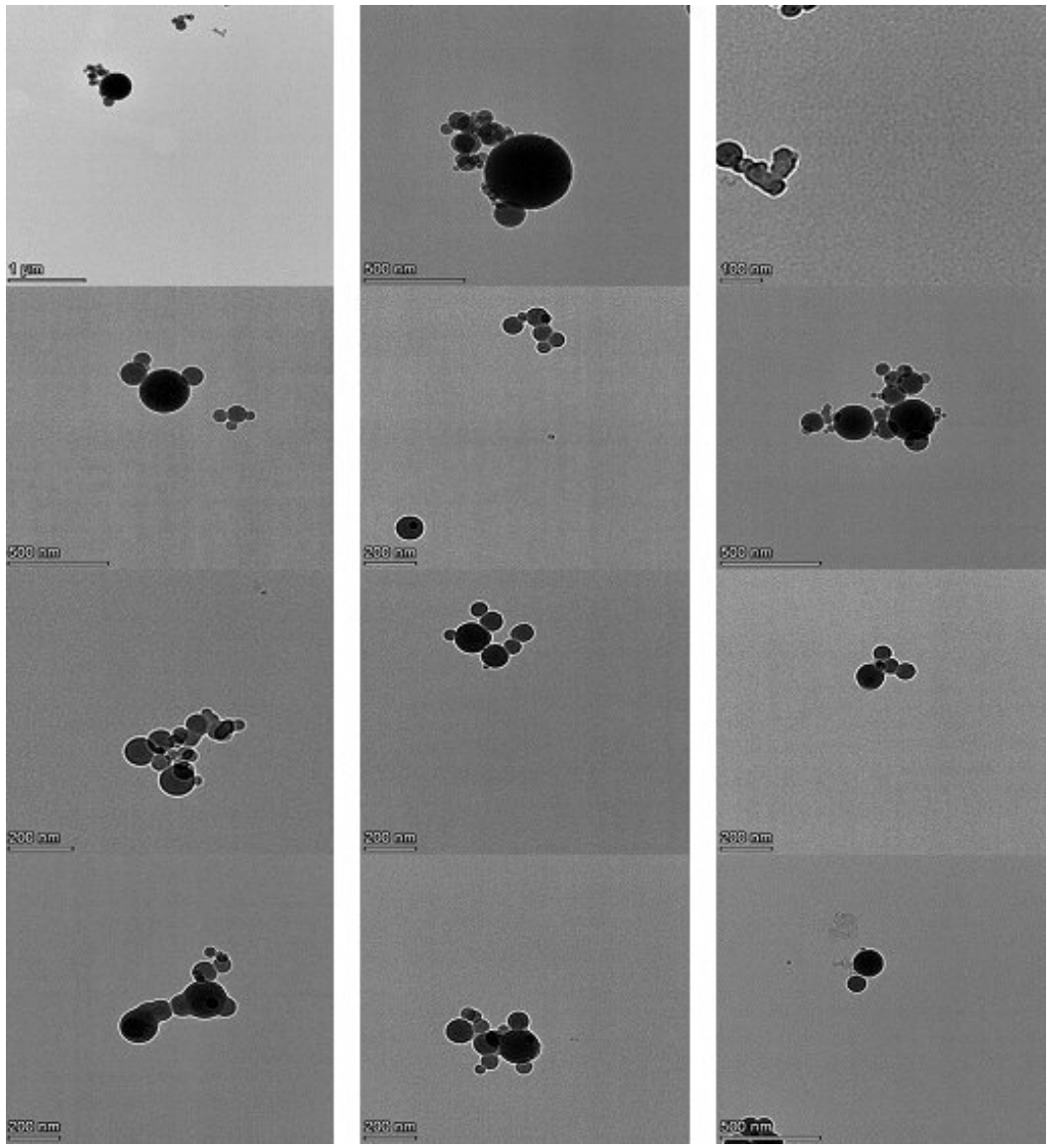

Fig. 4. TEM images showing the spherical morphology and aggregation of microsilica (amorphous SiO_2) nanoparticles.

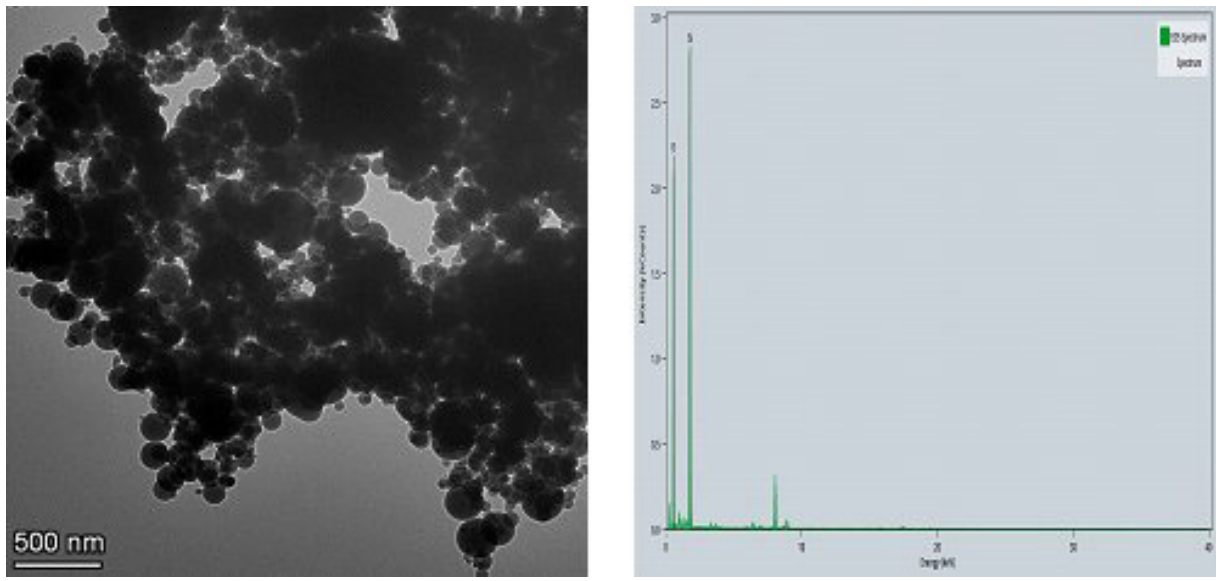

Fig. 5. TEM image of microsilica particles (scale bar: 500 nm) and the corresponding EDS spectrum.

Table 1. Comparison of microsilica properties with literature data.

Parameter	This study (Uzbekistan)	Zhong et al., 2019	Liang et al., 2023
SiO_2 content (%)	~ 99 (EDS)	92 - 97	90 - 95
Particle size (nm)	50 - 200	80 - 300	100 - 400
Morphology	Spherical	Spherical	Spherical
Structure	Predominantly amorphous	Amorphous	Amorphous

that the material was formed under comparatively stable process conditions. Such uniformity in particle size may be indicative of controlled vapor-phase nucleation and condensation dynamics during ferrosilicon production (Fig. 5).

The elemental composition of the sample was further examined by EDS at several selected points. The EDS spectra revealed only intense peaks corresponding to silicon (Si) and oxygen (O), with no significant signals from other elements.

Quantitative analysis showed that, in atomic percentages, O ≈ 64 at. % and Si ≈ 36 at. %, while in weight percentages, O ≈ 50.3 wt. % and Si ≈ 49.7 wt. %. These values are very close to the theoretical stoichiometric composition of SiO_2, thereby providing strong evidence that the sample consists almost entirely of silicon dioxide.

The TEM/SEM-EDS results are fully consistent with the previously obtained XRF, XRD, and FT-IR data. XRF analysis confirmed the predominance of silicon, XRD demonstrated the amorphous structural state, and FT-IR identified characteristic absorption bands corresponding to Si -O - Si bonds. Electron microscopy further substantiated these findings at the morphological level, revealing that the material is composed of amorphous, spherical, nanosized microsilica particles.

Overall, the TEM/SEM-EDS results allow the investigated material to be characterized as highly dispersed, spherical, amorphous SiO_2-rich microsilica (silica fume). Such a structure ensures a high specific surface area, enhanced reactivity, and favourable functional properties, indicating that the material is a promising secondary raw material for the production of binders, composite materials, adsorbents, and functional additives (Table 1).

CONCLUSIONS

The investigated microsilica sample was comprehensively characterized using complementary physicochemical and structural techniques, including XRF, XRD, FT-IR, and electron microscopy (TEM/

EDS). The integrated application of these analytical methods enabled the formulation of consistent and reliable scientific conclusions regarding the elemental composition, phase state, chemical bonding, and morphological features of the material.

XRF analysis demonstrated that silicon is the principal component of the sample (Si ≈ 50.6 wt. %). The presence of Ca, Al, Mg, K, Fe, Mn, and Zn confirms the metallurgical origin of the material and indicates the occurrence of silicate and aluminosilicate-associated phases. This compositional profile is characteristic of microsilica dust generated during ferrosilicon production.

XRD results revealed a broad diffuse maximum (amorphous halo) within the 2θ ≈ 15 - 30° range, with an almost complete absence of sharp crystalline peaks. This indicates that the sample predominantly exhibits an amorphous structure. The observed structural state is attributed to vapor-phase formation at high temperature followed by rapid cooling and condensation of SiO vapors into amorphous SiO_2.

FT-IR analysis confirmed the chemical structure of the material. The intense absorption bands observed at ~ 1100 cm^{-1} (asymmetric Si-O-Si stretching), ~ 800 cm^{-1} (symmetric stretching), and ~ 460 cm^{-1} (Si-O bending vibrations) are characteristic of amorphous silicon dioxide (SiO_2) and are fully consistent with the XRD and XRF findings. Additionally, the broad band ~ 3400 cm^{-1} indicates the presence of silanol (Si-OH) groups and adsorbed water.

TEM analysis provided detailed insight into the morphological characteristics of the sample. The particles were predominantly spherical, nanosized (typically 50 - 200 nm), and strongly aggregated. EDS analysis revealed that the material consists almost exclusively of Si and O, with atomic and weight ratios close to the theoretical values for SiO_2. These findings confirm that the sample is composed of highly pure amorphous silica.

The combined results of XRF, XRD, FT-IR, and TEM analyses consistently demonstrate that the investigated material is a technogenic microsilica (silica fume) composed mainly of amorphous silicon dioxide and spherical nanoscale particles. Such composition and structure provide a high specific surface area, enhanced reactivity, and favourable functional properties. Therefore, the material can be considered a promising secondary raw material to produce amorphous SiO_2, functional fillers, composite systems, and construction materials.

The scientific novelty of this study lies in establishing a correlation between the composition and structural characteristics of technogenic microsilica formed under specific technological conditions of ferrosilicon production. The presence of associated elements such as Ca, Fe, and Mn was shown to contribute to an increased degree of structural disorder (amorphousness) of silicon dioxide and a reduced concentration of silanol groups. These features distinguish the investigated microsilica from conventional silica fume samples and substantiate its scientific and practical potential as a functional filler material.

Authors' contributions

The initiators of the proposed article were S.K., I.Sh., O.B., S.M. and O.A. contributed significantly to the experimental section and the final manuscript. D.K. is responsible for checking the article, assessing the correctness of each process and introducing the basics. All authors considered the final manuscript in every possible way and made valuable additions. The authors contributed significantly to the article and confirmed the presented version.

REFERENCES

1. S. Zhu, C. Gao, J. Hu, W. Yu, H. You, Evaluation of steel metallurgical dust management: combining treatment methods and resource attributes, Process Saf. Environ. Prot., 191, B, 2024, 1648-1658. doi: 10.1016/j.psep.2024.09.052.
2. J. Zhang, Y. Zhang, Y. Long, C. Tian, P. Du, Q. Ren, Characterization of Physical and Chemical Properties of Multi-Source Metallurgical Dust and Analysis of Resource Utilization Pathways, Metals, 14, 12, 2024, 1378. doi: 10.3390/met14121378.
3. M.M. Yakubov, O.M. Yoqubov, D.B. Kholikulov, M.S. Maksudhodjaeva, Depletion of converter slags to waste in the Vanyukov furnace during pyrometallurgical copper production at JSC Almalyk MMC, Compl. Use of Min. Resour., 331, 4, 2024, 60-68. doi: 10.31643/2024/6445.39.
4. M-J. Kang, Y.K. Kwon, S. Yu, P-K. Lee, H-S. Park,

N. Song, Assessment of Zn pollution sources and apportionment in agricultural soils impacted by a Zn smelter in South Korea, J. Hazard. Mater., 364, 2019, 475-487. doi: 10.1016/j.jhazmat.2018.10.046.
5. D.B. Holikulov, R.I. Normurotov, M.I. Shonazarov, Extraction of precious metals from the magnetic fraction of gold processing plants by chlorination, Tsvetn. Met. (Moscow, Russ. Fed.), 1, 2025, 26-32. doi: 10.17580/tsm.2025.01.04.
6. A. Nikolov, V. Kostov-Kytin, M. Tarassov, L. Tsvetanova, N.B. Jordanov, E. Karamanova, I. Rostovsky, Characterization of Cement Kiln Dust from Bulgarian Cement Plants, J. Chem. Technol. Metall., 60, 3, 2025, 455-463. doi: 10.59957/jctm.v60.i3.2025.11.
7. R. Siddique, N.K. Chahal, Effect of silica fume on properties of concrete, Resour., Conserv. Recycl., 55, 8, 2011, 739-744. doi: 10.1016/j.resconrec.2011.03.004.
8. S. Zhong, J. Li, H. Ma, J. Niu, X. Shen, Chemical structure of amorphous Si-O in silica fume from ferrosilicon production, ISIJ Int., 59, 6, 2019, 1098-1104. doi: 10.2355/isijinternational.isijint-2018-516.
9. E. Kuzielová, M. Slaný, M. Žemlička, J. Másilko, M.T. Palou, Phase composition and reactivity aspects of silica fume, Materials, 14, 11, 2021, 2786. doi: 10.3390/ma14112786.
10. Y. Liang, H. Zhang, H. Ding, S. Sun, Y. Wang, X. Bai, S. Li, Amorphous silica prepared by byproduct microsilica in ferrosilicon production and applied in silica-TiO_2 composite, J. Mater. Res. Technol., 26, 2023, 235-245. doi: 10.1016/j.jmrt.2023.07.179.
11. Sh.T. Khojiev, D.B. Kholikulov, S.S. Mutalibkhonov, I.I. Shaymanov, G. Ma, Comparative thermodynamic analysis of fluxing additives Na_2O and CaO in iron recovery from silicate slag of ferrous metallurgy, Chern. Met., 9, 1125, 2025, 12-18. doi: 10.17580/chm.2025.09.026.
12. A. Crețu, C. Mattea, S. Stapf, I. Ardelean, The Effect of Silica Fume and Organosilane Addition on the Porosity of Cement Paste, Molecules, 25, 8, 2020, 1762. doi: 10.3390/molecules25081762.
13. J. Qin, X. Pang, H. Li, Z. Zhang, Mechanism of long-term strength retrogression of silica-enriched Portland cement, Front. Mater., 9, 2022, 982192. doi: 10.3389/fmats.2022.982192.
14. T. Zhou, J.-H. Hu, F.-W. Zhao, M.-M. Guo, S.-G. Xue, Effects of silica fume on the multi-scale material properties of composite Portland cement-based cutoff wall backfill, J. Cent. South Univ., 32, 2025, 205-219. doi: 10.1007/s11771-025-5868-8.
15. B. Uzbas, H. Akyildiz, Investigation of the effects of microsilica on arc sprayed coatings, Engineering, Eng. Technol. Appl. Sci. Res., 10, 3, 2020, 1066-1070. doi: 10.48084/etasr.3288.
16. I. Mitov, B. Yordanov, R. Gavrilova, V. Karadjova, Technological Possibilities for the Utilization of Iron-Containing Waste from Metallurgical Industries, J. Chem. Technol. Metall., 60, 3, 2025, 497-502. doi: 10.59957/jctm.v60.i3.2025.15.
17. T. Nochaiya, W. Wongkeo, A. Chaipanich, Utilization of fly ash with silica fume and properties of Portland cement-fly ash-silica fume concrete, Fuel, 89, 3, 2010, 768-774. doi: 10.1016/j.fuel.2009.10.003.
18. A.C.A. Müller, K.L. Scrivener, A.M. Gajewicz, P.J. McDonald, Use of silica fume to increase the density of C-S-H in cement paste, Cem. Concr. Res., 74, 2015, 116-125. doi: 10.1016/j.cemconres.2015.04.005.
19. H. Temiz, M. Karakeci, An investigation on microstructure of high-performance concrete, Cem. Concr. Res., 32, 7, 2002, 1131-1132. doi: 10.1016/j.cemconres.2015.04.005.
20. M. Saad, S.A. Abo-El-Enein, G.B. Hanna, M.F. Kotkata, Effect of silica fume on thermally treated concrete, Cem. Concr. Res., 26, 10, 1996, 1479-1484. doi: 10.1016/0008-8846(96)00142-1.
21. W. Wongkeo, P. Thongsanitgarn, A. Ngamjarurojana, A. Chaipanich, Compressive strength and chloride resistance of self-compacting concrete containing high level fly ash and silica fume, Mat. Des., 64, 2014, 261-269. doi: 10.1016/j.matdes.2014.07.042.
22. Y. Biskri, D. Achoura, N. Chelghoum, M. Mouret, Mechanical and durability characteristics of High-Performance Concrete containing steel fibers and silica fume, Constr. Build. Mater., 150, 2017, 832-838. doi: 10.1016/j.conbuildmat.2017.06.017.
23. A. Payzullaev, S. Mirzaev, M. Gafurova, S. Nurmatov, B. Allaev, Effect of Silica Nanoparticles on Water Evaporation Process, J. Chem. Technol. Metall., 60, 4, 2025, 625-630. doi: 10.59957/jctm.v60.i3.2025.15.
24. D. Kholikulov, Sh. Khojiyev, R. Mirzaxmedov,

A. Kambarov, R. Samariddin, The issue of metal extraction during ozonation purification of copper production process solutions, J. Chem. Technol. Metall., 61, 1, 2026, 175-181. doi: 10.59957/jctm.v61.i1.2026.20

25. S.G. Borisade, S.S. Owoeye, A. Ayeni, Synthesis and Characterization of Pure Amorphous Silicon Oxide from Treated Kaolinitic Clay Using Chemical Extraction, J. Chem. Technol. Metall., 59, 3, 2024, 613-622. doi: 10.59957/jctm.v59.i3.2024.15.
26. U. Yokubov, K. Egamberdiev, B. Allaev, O. Trunilina, S. Telyaev, M. Gafurova, Silica Nanoparticles Hydrosol for Concrete Strength Increase by Adding to Mixing Water, J. Chem. Technol. Metall., 58, 5, 2023, 932-936.
27. R. Chaid, P. Chahar, P. Sharma, D. Singla, Experimental study on high strength concrete containing micro silica and fly ash, Mater. Today: Proc., 14, 2019, 1152-1158. doi: 10.1016/j.matpr.2019.04.068.
28. J.M. Gao, C.X. Qian, B. Wang, K. Morino, Experimental study on properties of polymer-modified cement mortars with silica fume, Cem. Concr. Res., 32, 1, 2002, 41-45. doi: 10.1016/S0008-8846(01)00626-3.
29. M. Mazloom, A.A. Ramezanianpour, J.J. Brooks, Effect of silica fume on mechanical properties of high-strength concrete, Cem. Concr. Res., 26, 4, 2004, 347-357. doi: 10.1016/S0958-9465(03)00017-9.
30. F.N. Okoye, J. Durgaprasad, N.B. Singh, Effect of silica fume on the mechanical properties of fly ash based-geopolymer concrete, Ceram. Int., 42, 2, 2016, 3000-3006. doi: 10.1016/j.ceramint.2015.10.084.
31. M. Rostami, K. Behfarnia, The effect of silica fume on durability of alkali activated slag concrete, Constr. Build. Mater., 134, 2017, 262-268. doi: 10.1016/j.conbuildmat.2016.12.072.
32. K.S. Youm, J. Moon, J.Y. Cho, J.J. Kim, Experimental study on strength and durability of lightweight aggregate concrete containing silica fume, Constr. Build. Mater., 114, 2016, 517-527. doi: 10.1016/j.conbuildmat.2016.03.165.
33. B.-Q. Yan, D.D. Tannant, F.-H. Ren, M.-F. Cai, Effects of silica fume on the performance of cemented paste backfill mixed with brine, Geotech. Geol. Eng., 37, 5, 2019, 4575-4587. doi: 10.1007/s10706-019-01011-y.
34. T. Gupta, S. Chaudhary, R.K. Sharma, Mechanical and durability properties of waste rubber fiber concrete with and without silica fume, J. Cleaner Prod., 112, 2016, 702-711. doi: 10.1016/j.jclepro.2015.07.081.
35. S. Cao, D. Zheng, E. Yilmaz, Z.Y. Yin, G.-L Xue, F.-D. Yang, Strength development and microstructure characteristics of artificial concrete pillar considering fiber type and content effects, Constr. Build. Mater., 256, 2020, 119408. doi: 10.1016/j.conbuildmat.2020.119408.
36. S. Kumar, R. Kumar, S.P. Mehrotra, Influence of granulated blast furnace slag on the reaction, structure and properties of fly ash based geopolymer, J. Mater. Sci., 45, 3, 2010, 607-615. doi: 10.1007/s10853-009-3934-5.
37. R.P. Williams, R.D. Hart, A. van Riessen, Quantification of the extent of reaction of metakaolin-based geopolymers using XRD, SEM and EDS, J. Am. Ceram. Soc., 94, 8, 2011, 2663-2670.
38. S. Zhao, Q. Zhang, Effect of Silica Fume in Concrete on Mechanical Properties and Microstructure, Materials, 12, 19, 2019, 3263. doi: 10.3390/ma12193263.
39. A. Mehta, D.K. Ashish, Silica fume and waste glass in cement concrete production: A review, J. Build. Eng., 29, 2020, 100888. doi: 10.1016/j.jobe.2019.100888.
40. A. Kar, Silica fume as filler in polymer composites (case studies), Polym. Compos., 2023. doi: 10.1002/pc.27877.
41. A.S. Raja, A. Kumaravel, Silica fume reinforced polymer composite (filler effect), J. Reinf. Plast. Compos., 2015. doi: 10.1177/096739111502300608.